

# Residual stress measurements on a cut-welded Al-Ti plate using neutron diffraction techniques

M. Cabibbo, S. Marrone, E. Quadrini

*The nature and effect of residual stress on cut-weld Al-Ti plane disc was studied by means of neutron diffraction techniques. The study was extended from the parent aluminium-manganese-magnesium AA3003 alloy to the weld Al-Ti interface and then to the parent commercially pure titanium alloy. For this study, pulse neutron diffraction technique was applied. The residual stress level resulted practically weak within the two parent materials. Yet, it was found that the mean strain level suddenly increased in correspondence to the diffusion affected zone due to the cut-welding process. Microstructure diffusion processes within a narrow weld interface zone were investigated by scanning electron microscopy and energy dispersive spectrum techniques.*

**Keywords:** aluminum and alloys, titanium and alloys, welding, diffraction, technologies

## INTRODUCTION

The major advantages of using and develop the cold-roll cut-welding technology lie in the following principal metallurgical aspects: i) it is a solid state process which gives reproducibility and high-quality standards of the welds; ii) no filter wire, shielding gas or material supply is required; iii) no fume or spatter is produced; iv) less material is lost compared to other more diffuse welding techniques (e.g. flash welding) [1-10]. The pressures exerted by the rollers involve the depth of rolling and, consequently, the goodness of the welding process; moreover, it generates surface tensional states which, from point to point, are either negative (tension) or positive (compression) [1-7]. During cold-rolling, the dept of inter-diffusion phenomena have a strong effect on the welding process. A sufficient deep diffusion layer within each plate guarantees a strong bonding along the entire welded plate interface. [8-10].

Neutron diffraction is rather similar to the more familiar and common X-ray diffraction used for microstructure characterisation in materials science field. The use of neutron, instead of X-ray sources, involves a major advantage in terms of penetration depth of neutrons within the metallic material, which allows the mapping of lattice parameter variations as a function not only of lateral position, as the case of X-ray diffraction, but also of different thickness layers in the interior of bulk materials [11-20]. With this respect, the development of the neutron diffraction technique and its applicability to bulk engineering components has largely and more and more been driven by its peculiar ability to measure a macro-scale level stress field, as a non-destructive mean. Moreover, the use of neutron diffraction is increasing within the materials scientist community as a powerful mean to validate models and thus aid life predictions and the development of failure criteria [11-16, 20]. The use of pulse and elastic neutron diffraction techniques to determine lattice parameter variations, or d-spacing, as a result of internal residual elastic strains, is well established [16-19]. By means of dif-

fraction technique, components of strain are measured directly from changes in crystal lattice spacing. When illuminated by radiation of wavelength very close to the material interplanar spacing, crystalline materials diffract the incident radiation generating distinctive Bragg-peaks. The angle at which any given peak occurs can be thus calculated using Bragg's law for diffraction. In particular, using thermal neutrons the penetration depth in the most common metallic material is usually a thousand time deeper compared to common X-ray sources (Cu, Cr or Mo cathode sources involving wavelengths of respectively: 0.154, 0.229, 0.071 Å) [17-19]. Consequently, neutron diffraction is suitable for investigating strains within bulk specimens, the obtained strain being an average over the entire gauge volume (that is the volume over which the neutrons scatter from). Strains, obtained from single peaks, are thus used to evaluate the macroscopic strain-field.

This paper aimed at illustrating a microstructure investigation on a cut-weld Ti-Al interface. The inter-diffusion profile was acquired by means of scanning electron microscopy (SEM) and energy dispersive spectrum (EDS) techniques. Residual stress in the weld zone was evaluated by means of neutron diffraction techniques.

## EXPERIMENTAL AND METHOD

The cold-roll welding process was applied to two plates: a commercially pure titanium and the aluminium-manganese-magnesium 3003 alloy, whose chemical composition is shown in Table 1. The Al holed plate had a diameter of 82 mm, and the small Ti-plate had a diameter of 8 mm. Before welding, Ti and Al surfaces were mechanical pickled to reduce and, eventually, eliminate the oxides layer in Al and Ti surface being welded [7]. For microstructure investigations of inter-diffusion layers, specimens were simply mechanical ground and then polished to 0.25 µm diamond paste. Investigations were carried out by means of a scanning electron microscope (Philips XL30) using the back-scattered electron (BSE) signal. X-ray EDS was used to calculate the weight percent of respectively Al within the Ti plate and Ti in the Al plate along the weld surface, together with diffusion profile mapping along a path normal to the weld interface. Different Al-Ti cut-welded plates were produced and investigated.

Marcello Cabibbo, Simona Marrone, Enrico Quadrini

INFM / Dipartimento di Meccanica, Università Politecnica delle Marche, Ancona, Italy

Paper presented on 25 June 2004

Residual stress measurements were carried out by means of neutron diffraction at the E3 diffractometer of the HMI-BENSC, Berlin. The neutron wavelength was 1.370 Å and the investigated peaks were Al-(200) and Ti-(111). By measuring the flight times of diffracted neutrons, their wavelengths are calculated and the diffracted spectra recorded. The incident spectra are polychromatic, thus all possible lattice planes are recorded at each measurement. The scattering vectors for all the recorded reflections lie basically in the same direction, and thus measurements of the strain come from the same direction. Each reflection is produced from a different family of grains, oriented such that the specific (hkl) plane diffracts to the detector. Thus, strain can be determined from the shift in a given reflection. Yet, since an entire diffraction spectrum is obtained for each measurement direction, strain is determined directly from the whole diffraction data using the Rietveld [18] method, in which a crystallographic model of the structure is fitted to the entire diffraction spectrum. As a fixed scattering angle is used, radial focussing collimator is used to let neutrons be detected over a wider solid angle than if by using traditional slit. This configuration can ensure all collected neutrons to come from the a

defined sample volume [19]. In the adopted configuration, two radial collimators allow two perpendicular strain directions to be measured simultaneously. This configuration also enables to build-up a map of strain as a function of position within the sample, just by defining the gauge volume within the sample and moving the sample relative to the beam and detectors. For all the strain measurements, it was assumed the strain to be independent of position within a given xz-plane, provided the gauge was not too close to the sample edge. Residual stress measurements were extended to the hoop, radial and axial direction of the weld.

RESULTS AND DISCUSSION

a) Diffusion interface analysis and fracture mechanism

Figure 1 shows the diffusion profile of Ti-Al cut welded plates acquired by means of EDS technique. The inter-diffusion penetration depth was ~1.8 µm, for Ti into Al, and up to ~10 µm for Al into Ti. The attached light-microscopy (LM) micrographs show the microstructure of the cut-welded profile, from the parent Al to the parent Ti plate passing through the

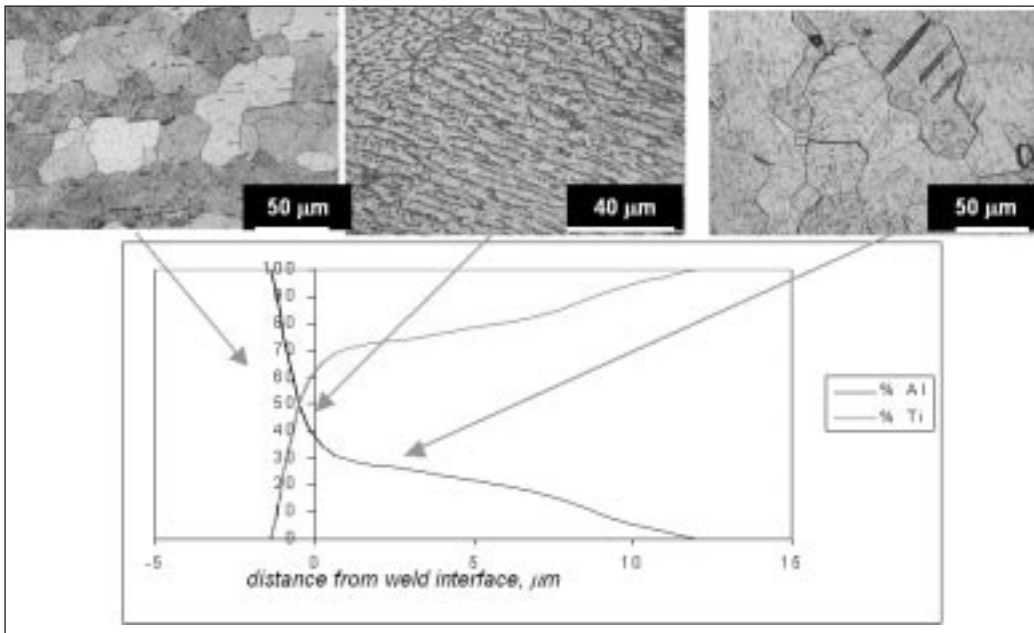


Fig. 1 – Diffusion Interface profile of 1L heat treated at 300°C/5h. Al (black line), Ti (grey line). LM micrographs show the microstructure of the Al parent, Al-Ti welded zone and Ti parent material, respectively.

Fig. 1 – Profilo di interdiffusione del materiale 1L sottoposto a trattamento termico a 300°C/5h. Al (linea nera), Ti (linea grigia). La micrografia mostra la microstruttura del materiale base di alluminio, la zona saldata Al-Ti e il metallo base di titanio.

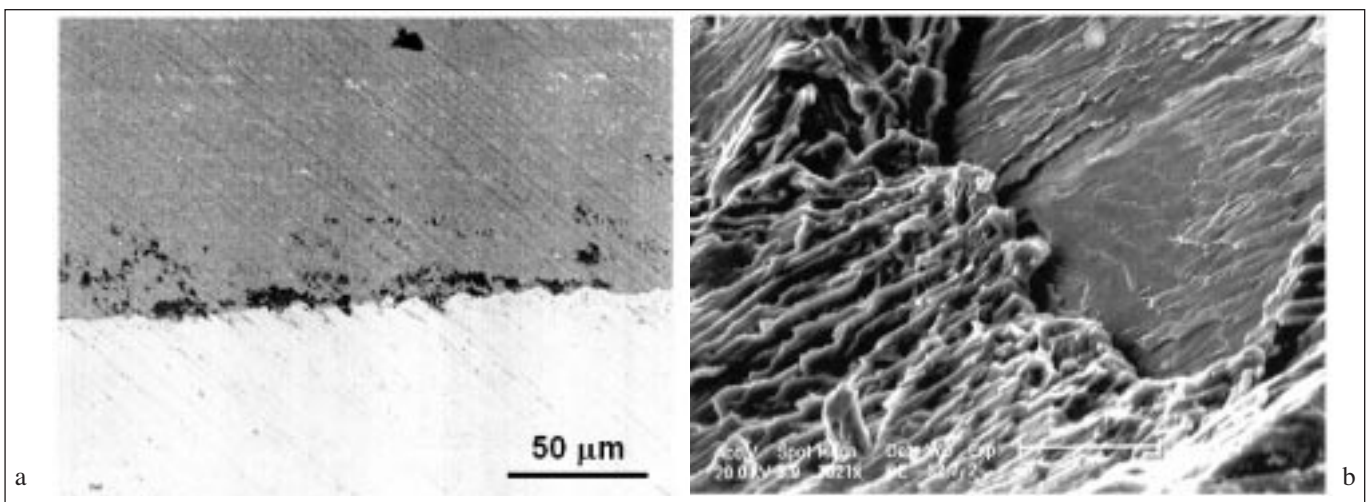


Fig. 2 – LM image of partly welded plate (upper side Ti, lower side Al) (a). SEM image of a typical transient zone from ductile to brittle fracture (b).

Fig. 2 – Micrografia al microscopio ottico di un laminato parzialmente saldato (parte superiore Ti, parte inferiore Al) (a). Immagine SEM (microscopia elettronica in scansione) di una tipica zona di frattura da duttile a fragile (b).

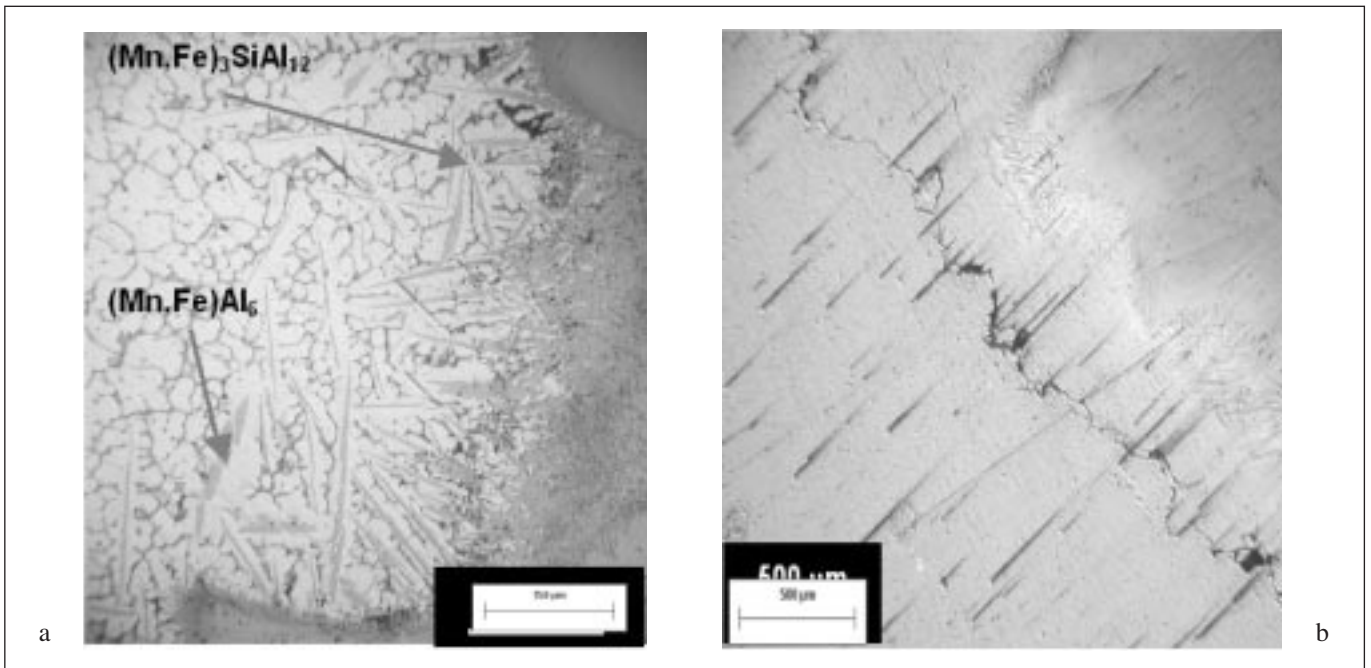


Fig. 3 – LM image of the weld within the parent Al-plate (a), EDS analysis identified the arrowed particles as  $(Mn,Fe)Al_6$  and  $(Mn,Fe)_3SiAl_{12}$ . Ti-Al weld interface illustrating a propagating crack (b).

Fig. 3 – Immagine della saldatura all'interno de metallo base di alluminio (a), l'analisi Energy-Dispersive-Spectrum (EDS) ha permesso l'identificazione delle seguenti fasi secondarie:  $(Mn,Fe)Al_6$  and  $(Mn,Fe)_3SiAl_{12}$ . In (b) è illustrato il meccanismo di propagazione della microcricca lungo l'interfaccia di saldatura Ti-Al.

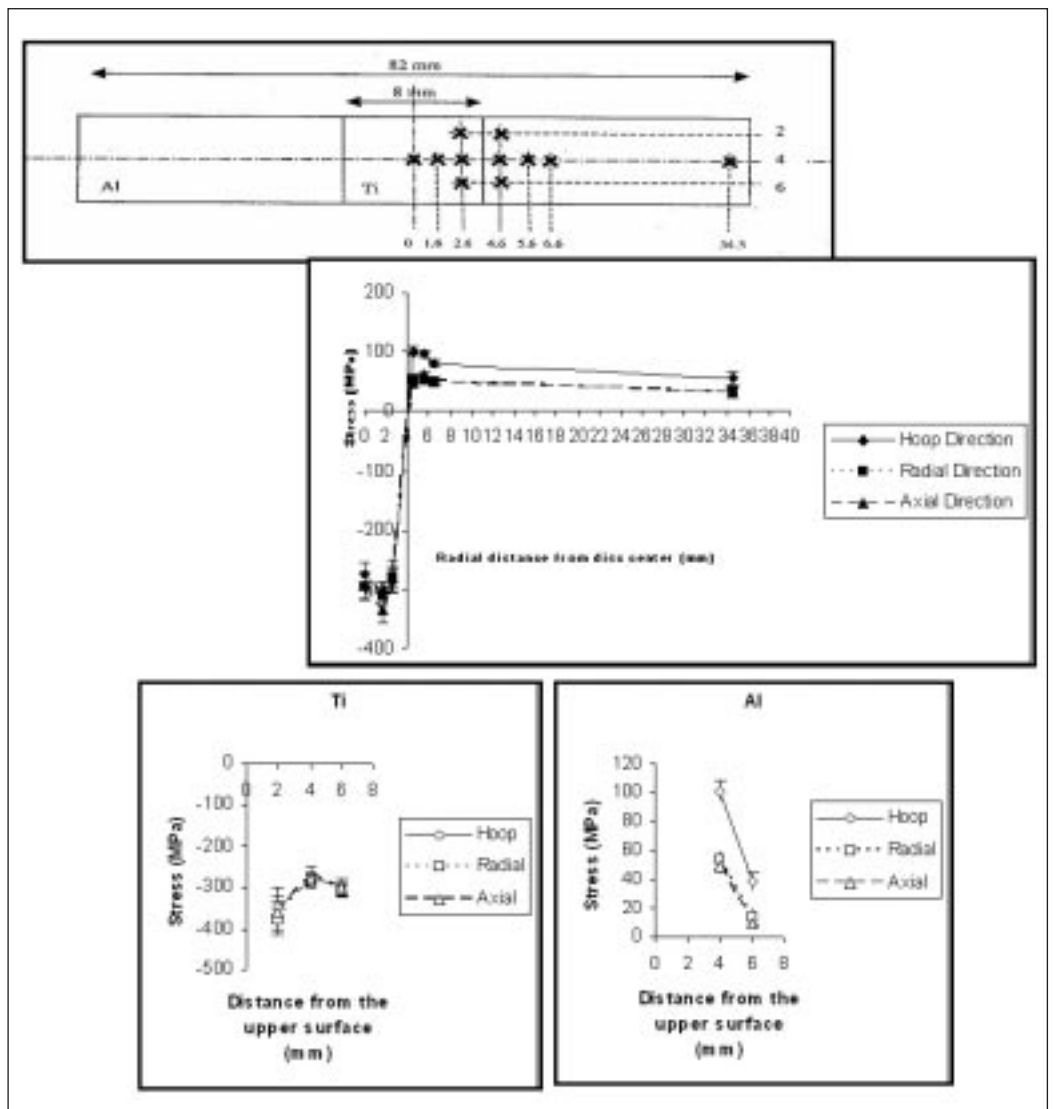


Fig. 4 – Hoop, radial and axial residual stress measurements acquired along the transverse section of the weld (top and middle of figure). In the bottom part of the figure the corresponding measurements along the axial direction of the weld within Ti (left) and within Al (right) are reported.

Fig. 4 – Misure di tensioni residue nella zona sommitale, radiale e assiale del giunto saldato, effettuata lungo la sezione trasversa. La parte inferiore della figura mostra le misure relative alla direzione assiale della saldatura all'interno del Ti (sinistra) e Al (destra).

weld zone in which the usual grained microstructure seemed to be lost.

Some welded plate experienced interfacial cracking and sometimes a consistent de-bonding along the welded surfaces during mechanical tensile tests and technological close bend tests (unpublished results). SEM fracture investigations and EDS analysis allowed to establish the nature and causes of cracking. Al-3003 alloy appeared to have a higher microvoids presence compared to commercially pure Ti. Indeed, the higher volume fraction of micro-voids in Al is also attributing to the alloying elements in Al compared to a higher purity level in Ti. Micro-voids volume fraction difference showed a different tensional response of the two plates following the cold roll process: a different surface tension stress is present along the welded region causing a state of residual stress responsible for possible cracking initiations. Figure 2 (a) is a representative image of a partly welded plate (upper side Ti, lower side Al). Figure 2 (b) reports a typical fracture which the cut-welded Al-Ti system was affected to. Very often, a transient zone from ductile to brittle fracture occurred in the very neighbouring of the weld interface and particularly within the parent Al material. It is believed that the strong tangle component of surface stress was responsible for the crack initiation through micro-voids segregation. Along the Al weld surface, and in a neighbouring strip region of 0.8 – 1.3 μm, a noticeable presence of precipitates was also detected (indicated in figure 3 (a)). The presence of the second phases has a detrimental effect on the diffusion of the welded plate because contributes to lower down the Al atoms available for the inter-diffusion in the weld zone, and consequently lowering the welded surface quality. EDS analysis allowed to identify the nature of the detected second phases to be (Mn,Fe)Al<sub>6</sub> and (Mn,Fe)<sub>3</sub>SiAl<sub>12</sub>. Small and diffuse cracks were also present in the next neighbouring of second phase particles, in someone of the cut-welded plates (Figure 3 (b)).

**b) Residual stress measurements**

Figure 4 shows the measured residual stress across the welded zone. The stress showed the same trend unrespectable of the direction along to which the diffraction was acquired (hoop, radial or axial). Within the parent Ti material, stresses are all of compression, and the value in the mid part of the parent Ti-plate and at the welding interface was ~280 MPa, while the maximum stress value of 305 MPa was recorded at a distance of 1.6 mm from the welded interface. Within the parent Al-material, hoop, radial and axial stresses were 100, 54, 49 MPa, respectively. The latter value was recorded at a distance from the welding interface of 4.6 mm and it was the minimum stress value across the entire welded affected zone. From this distance on, the residual stress continuously decreases until reaching values quite negligible.

**CONCLUSIONS**

The microstructure and residual stress state of a cold-roll commercially pure Ti-Al (3003) welded plate were investigated. SEM-EDS analyses were carried out to evaluate the diffusion profile normal to the weld interface. The diffusion depth was ~1.8 μm, for Ti into Al, and up to ~10 μm for Al into Ti.

Along the Al weld surface, and in a neighbouring strip region of 0.8 – 1.3 μm, a noticeable presence of precipitates was also detected and EDS analysis identified them as (Mn, Fe)Al<sub>6</sub> and (Mn,Fe)<sub>3</sub>SiAl<sub>12</sub>. Small and diffuse cracks were also present especially in the next weld interface neighbouring within the parent Al-plate.

Residual stress measurements showed a common curve sha-

Pb	Mn,Al, Ni, Si, Cr, Fe, Zn	Ti		
0.01	0.24 max (a)	99.75		
Mn	Mg	Fe	Si, Cu	Al
1.1	1.0	0.35 max (b)	0.32 max	97.2

Table 1 – Chemical composition of the commercially pure Ti (a) and Al 3003 (b), %wt.

Tabella 1 – Composizione chimica del titanio commercialmente puro (a) e della lega Al 3003 (b), %wt.

pe and similar values weather the diffraction was performed along the hoop, radial or axial cut-welded plate direction. The stress in the major part of the weld zone belonging to the Ti-plate was ~280 MPa, while the maximum stress value was of 305 MPa at a distance of 1.6 mm from the weld interface. Within Al-material, residual was about one-third and the minimum value of ~50 MPa was found at a distance of 4.6 mm from the welding interface.

**ACKNOWLEDGMENTS**

Experiments at HMI-BENSC were financed by European Commission (TMR/LSF Programme).

**REFERENCES**

- [1] Diffusion Bonding 2, D. J. Stephenson (Ed.), UK, 1991.
- [2] K. Thomas, “Cold Welding”, M. Petri, G. Petri (Eds.), ASM Handbook, 6, Welding, Brazing, Soldering, 1993.
- [3] L. De Chiffre, “Cut Welding Variants and Applications”, Welding Review Int’l, 1993.
- [4] W. Lehrheuer, Forschungszentrum Jülich GmbH, “High-Temperature Solid State Welding”, R.G. Lagi (Ed.), ASM Handbook, 6, Welding, Brazing, Soldering, 1993.
- [5] S.B. Dunkerton, “Procedure Development and Practice Considerations for Diffusion Welding”, The Welding Institute, ASM Handbook, 6, Welding, Brazing, Soldering, 1993.
- [6] W. Zhang, “Bond Formation in Cold Welding of Metals”, Technical University of Denmark, 1994.
- [7] M. Cabibbo and E. Quadrini, “Mechanical Properties of a Cu(DHP) - Al(3003) cold roll welded plate”, Materials Engineering, EDITEQ, 13, 2, 2002, 167.
- [8] R.S. Rosen, “Low-Temperature Solid State Welding”, ASM Handbook, 6, Welding, Brazing, Soldering, 1993.
- [9] Aluminium Alloys '90, Conference on Aluminium Alloys, Beijing, China, Int’l Academic Publishers, 1990.
- [10] S. Kalpakjian, “Manufacturing Engineering and Technology”, Addison Wesley, 1989.
- [11] G. Albertini, G. Bruno, F. Fiori, E. Girardin, A. Giuliani and E. Quadrini, “X-ray and neutron diffraction determination of residual stresses in a pressed and welded component”, Physica B, 276-278, (2000), 876.
- [12] G. Albertini, G. Bruno, B.D. Dunn, F. Fiori, W. Reimers and J.S. Wright, “Comparative neutron and X-ray residual stress measurements on Al-2219 welded plate”, Mater. Sci. Eng. A, A224, (1997), 157.
- [13] C. Hsu and C.E. Albright, “Fatigue analysis of laser welded lap joint”, Eng. Fract. Mechanics, 39, 3, (1991), 575.
- [14] G. Buss and P.E. Irving, “The role of residual stress and heat affected zone properties on fatigue crack propaga-

- tion in friction stir welded 2024-T351 aluminium joint", *Int. J. Fatigue*, 25, (2003), 77.
- [15] A.P. Reynolds, W. Tang, T. Gnaupel-Herold and H. Prask, "Structure, properties, and residual stress of 304L stainless steel friction stir welds", *Scripta Mater.*, 48, (2003), 1289.
- [16] I.C. Noyan and J.B. Cohen, "Residual stress, measurement by diffraction and interpretation", Springer, New York, 1987.
- [17] H.M. Rietveld, *J. Appl. Cryst.*, 2, (1969), 65.
- [18] P.J. Withers, M.W. Johnson and J.S. Wright, "Neutron strain scanning using a radially collimated diffracted beam", *Physica B*, 292, 3-4, (2000), 273.
- [19] H. Wohlfahrt, in: E. Macherauch, V. Hauk (Eds.), "Residual stress", DGM Verlag, Oberursel, 1983.
- [20] Proceedings of the NATO Adv. Res. Workshop on Measurement of residual stress using neutron diffraction, Oxford, March 1991, Kluwer Academic Publishers, Dordrecht, 1992.

A B S T R A C T

**MISURE DI TENSIONI RESIDUE IN UN LAMINATO AL-TI  
SALDATO A FREDDO  
MEDIANTE TECNICHE DI DIFFRAZIONE NEUTRONICA**

**Parole chiave:** alluminio e leghe, titanio e leghe, saldatura, diffrattometria, tecnologie

La natura microstrutturale e gli effetti sulle tensioni residue generate dalla saldatura di un disco Al-Ti sono state studiate rispettivamente mediante microscopia ottica, elettronica e diffrazione neutronica. Lo studio non si è limitato alla sola zona di saldatura ma ha coinvolto anche i due materiali base: Al e Ti. Il primo è una lega Al-Mn AA3003, il secondo è titanio commercialmente puro. In particolare, per lo studio delle tensioni residue, si è adottata la tecnica di diffrazione

neutronica ad impulsi con frequenza e pacchetti di energia ottimizzati. Il livello pensionale lungo i due materiali base è risultato essere praticamente costante e a debole intensità. Tale livello ha registrato un repentino innalzamento in corrispondenza della zona di interdizione tra Al e Ti. Il profilo di interdizione, peraltro generato dalla saldatura stessa e sintomo di una buona aderenza tra i due materiali saldati a freddo, è stato caratterizzato mediante microscopia elettronica e correlato al profilo di tensioni residue registrato mediante diffrazione. L'intero processo di interdizione è stato caratterizzato mediante Energy-Dispersive-Spectrum con il quale, talaltro, è anche stato possibile determinare la natura delle seconde fasi che sono precipitate durante riscaldamento a 300°C/5h post saldatura a freddo. Tali fasi sono:  $(Mn,Fe)Al_6$  and  $(Mn,Fe)_3SiAl_{12}$ .